

Newtonian Modeling of Second-Generation FACTS Devices using Unaltered Power-Flow Routines

Gorazd Bone, Miloš Pantoš, *Member, IEEE* and Rafael Mihalič, *Member, IEEE*

Abstract-- This paper proposes a Newtonian method for Power Flow (PF) calculations that incorporates second-generation Flexible Alternating Current Transmission System (FACTS) devices without altering the standard PF routines. The method constructs a criterion function that is external to the PF routine, and which has the property of becoming zero when the FACTS devices are correctly modeled. The external character of the criterion function and the property of becoming zero at the correct solution are used to form the FACTS-device modeling problem as an external root search, i.e., it occurs externally to the PF. The Newton method is used for the root search, which provides for a Newtonian convergence character of the proposed method, and so convergence is achieved within a few iterations. By using numerically obtained sensitivities it is shown that the method easily incorporates different control modes into the modeled FACTS devices—a property that will prove beneficial with the development of smart grids. The method is tested by modeling configurations with single and multiple FACTS devices on the benchmark IEEE300 and Pegase13659 systems

Index Terms-- Newton method, Power flow control, Power flow, Sensitivity analysis

I. INTRODUCTION

THE power-flow (PF) study is one of the most fundamental analyses of Electrical Power Systems (EPS) as it provides both detailed information about the steady-state operation and initial values for dynamical simulations of the EPS. Since controllable devices, such as phase- and tap-changing transformers or Flexible Alternating Current Transmission System (FACTS) devices, affect the EPS, the PF algorithm used to analyze a given EPS must be able to consider the effects of any controllable devices that are present. Adapting the PF algorithm to consider all types of controllable devices is not a trivial task, since each type of device alters the system of equations that describe the EPS in a unique way.

The fact that the PF must be altered accordingly for each type of controllable device creates inconveniences when

developing new algorithms, as practical applications must wait until modeling the relevant devices has also been researched for the specific algorithm. This becomes clear if we compare, for example, the well-established Newton Raphson (NR) PF [1] to the more recent Holomorphic Embedding (HE) PF [2]. The two algorithms are fundamentally different and modeling controllable devices for the HE-type PF is being researched [3], [4], [5], while there already exist modeling techniques for the NR PF [6], [7], [8]. While the HE method exhibits better convergence than its NR counterpart [9], the practical usage of this method will have to wait until all the relevant controllable devices have been applied.

Additional difficulties when modeling controllable devices can arise from the application of smart-grid technologies. Smart-grid development concerns adding measurements in an EPS—providing Power System Operators (PSO) with detailed information about the system, while adding communication channels—enabling the PSO to influence the operation of controllable devices in the EPS. Smart grids thus enable the PSO to use controllable devices in different ways, which could be more beneficial for EPS operation. For example, an SSSC, which usually controls the active power flow through its line, could be used to bring the line current of a nearby line, or a voltage magnitude of a nearby node, below the maximum limit. As altering control modes becomes possible and beneficial for the EPS, future modeling tools must be able to incorporate unforeseen control modes easily.

The methods that model controllable devices generally alter the underlying PF routine, since controllable devices are usually regarded as direct expansions of the original PF problem. This has the consequence that adding the modeling capability for a new type of controllable device to existing PF software requires that the software is fundamentally changed. Additionally, as the equations are usually hard-coded in the source code, fundamental changes must also be made if new control modes are being added.

In this paper a Newtonian method to model second-generation FACTS devices in PF studies is proposed. The method has the characteristic that the devices are modeled externally to the PF routine. To achieve the external character, the method relies on using the load equivalent for second-generation FACTS [10], [11], and presenting the conditions related to the modeling as an external criterion function (external with respect to the PF routine); when the criterion

Manuscript received on February 12., 2018

G. Bone is with the Laboratory of Electric Power Supply, University of Ljubljana, Faculty of Electrical Engineering, SI-1000 Ljubljana, Slovenia (e-mail: gorazd.bone@fe.uni-lj.si)

M. Pantoš is with the Laboratory of Power Systems, University of Ljubljana, Faculty of Electrical Engineering, SI-1000 Ljubljana, Slovenia (e-mail: milos.pantos@fe.uni-lj.si).

R. Mihalič is with the Laboratory of Electric Power Supply, University of Ljubljana, Faculty of Electrical Engineering, SI-1000 Ljubljana, Slovenia (e-mail: rafael.mihalic@fe.uni-lj.si)

function's entries are zero, the value of the load powers correctly represents the FACTS devices. The external character enables the modeling of controllable devices without changing the PF routine. The modeling task is reduced to an external root search. This makes the method applicable to any type of PF. Additionally, adding control modes with the presented method is achieved by altering only the routine that models the devices, while the underlying PF routine remains unchanged. The Newton method is used to find the root of the criterion function. Tests show that the proposed method converges within a few iterations.

The presented method was previously successfully tested on the SSSC in [12] and on tap-changing, phase-shifting and quadrature-boosting transformers in [13]. In [13] it is shown that the method can also incorporate changing impedances of the modeled devices.

The rest of the paper is organized as follows: a detailed explanation of the method, the criterion function development for each type of the device and a detailed explanation of the procedure are presented in Section II; while Section III presents the numerical results; and the conclusion is drawn and some remarks are made in Section IV.

II. METHOD DEVELOPMENT

The proposed method uses the concept of representing the voltage sources of FACTS devices with equivalent load powers, which are the inputs of a PF. The aim of the method is essentially to find the values of the load powers that will correctly represent the FACTS devices. The load powers must therefore be bound to the correct values in a way that considers the functionality of modeled FACTS devices.

To bind the load powers to their correct value we construct a criterion function; this is a vector function with the characteristic that all its entries are equal to zero when the load powers correctly model the FACTS devices for a given problem. Each entry of the criterion function represents some physical characteristic of a certain FACTS device. Since the modeling task is reduced to finding the values of load powers that will force the values of the criterion vector function to be zero, the method turns the problem of modeling controllable devices into that of a root search. As the characteristic vector function is built externally to the underlying PF routine, this root search is performed externally to the PF, and so the PF can remain unchanged. To find the root of the criterion function the Newton method is used, which provides for rapid convergence (usually within fewer than 10 iterations).

The remainder of this section is organized as follows. The load equivalent of the FACTS devices is revised in subsection A. This is followed by the development of the criterion function entries for the considered devices in subsection B. The root search using the Newton method is detailed in subsection C. Subsection D explains how to implement other control modes, how this changes the equation system and the derivatives used by the Newton search and how to derive the expressions. Considering the limitations is explained in subsection E. Lastly, subsection F discusses the unforeseen control modes, why they will likely arise in the future and how

to easily implement them using numerically obtained sensitivities.

A. Representing 2nd-generation FACTS by load powers

Steady-state representations of StatCom, SSSC and UPFC are various topologies of voltage sources [7], shown in Fig. 1.

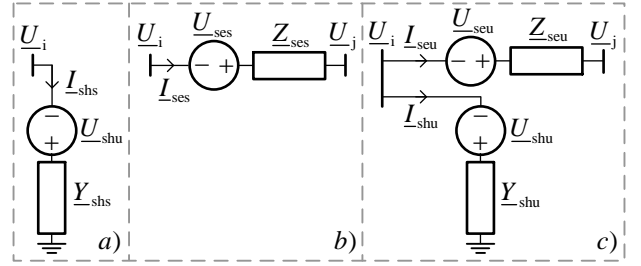


Fig. 1 : Voltage-source models for second-generation FACTS, a) StatCom, b) SSSC and c) UPFC.

In Fig. 1, Z_{seu} and Z_{ses} are series impedances of the UPFC and SSSC, Y_{shu} and Y_{shs} are shunt admittances of the UPFC and StatCom, I_{seu} and I_{ses} are currents of the series branch of the UPFC and SSSC, I_{shu} and I_{shs} are currents of the shunt branch of the UPFC and StatCom, U_{shu} and U_{shs} are voltages of the shunt source of the UPFC and StatCom, U_{seu} and U_{ses} are voltages of the series source of the UPFC and SSSC, and U_i and U_j are nodal voltages of nodes “i” and “j”, respectively.

To represent the voltage sources belonging to 2nd-generation FACTS devices by load powers, the Norton equivalent of the voltage sources is taken first. The current of the current source is then regarded by the respective power.

For *StatCom* this procedure is detailed in Fig. 2; the original circuit is shown in a), the Norton equivalent in b) and the load model in c). The equations that connect the load model to the original voltage source representation are (1), (2) and (3). Equation (4) provides the current flowing through the device, which is needed to derive the active power production of the device (see (16)).

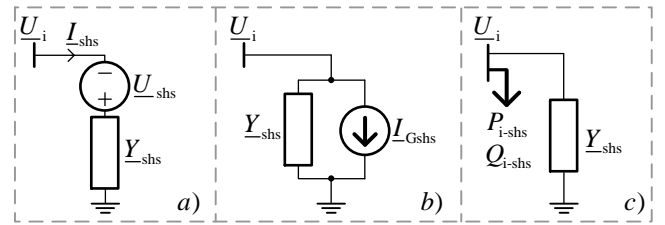


Fig. 2: Developing the StatCom load model.

$$I_{Gshs} = U_{shs} \cdot Y_{shs} \quad (1)$$

$$P_{i-shs} = \text{Re}\{I_{Gshs}^* \cdot U_i\}, \quad Q_{i-shs} = \text{Im}\{I_{Gshs}^* \cdot U_i\} \quad (2)$$

$$U_{shs} = (P_{i-shs} - j \cdot Q_{i-shs}) / (Y_{shs} \cdot U_i^*) \quad (3)$$

$$I_{shs} = (U_i + U_{shs}) \cdot Y_{shs} = \left(U_i + \frac{P_{i-shs} - j \cdot Q_{i-shs}}{Y_{shs} \cdot U_i^*} \right) Y_{shs}, \quad (4)$$

where P_{i-shs} and Q_{i-shs} are the active and reactive load power equivalents of the StatCom, respectively

To develop the load representation for the SSSC device a

similar procedure is followed. Since the Norton current source is connected between two nodes, the load power model for the SSSC requires four loads (active and reactive load powers at each of the two nodes). The procedure is detailed in Fig. 3, with the original circuit in a), the Norton equivalent in b) and load model in c). The equations relating the voltage source model to the load power equivalent are (5), (6) and (7). The device's current is provided in (8) and is necessary to derive the active power production (see (18)) of the SSSC and the active power flow (see (19)) through the SSSC.

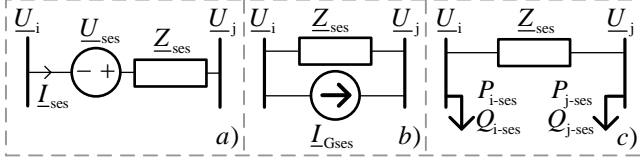


Fig. 3: Developing the SSSC load model.

$$I_{Gses} = \underline{U}_{ses} / Z_{ses} \quad (5)$$

$$P_{i-ses} = \text{Re}\{I_{Gses}^* \cdot \underline{U}_i\}, \quad Q_{i-ses} = \text{Im}\{I_{Gses}^* \cdot \underline{U}_i\} \quad (6)$$

$$P_{j-ses} = \text{Re}\{-I_{Gses}^* \cdot \underline{U}_j\}, \quad Q_{j-ses} = \text{Im}\{-I_{Gses}^* \cdot \underline{U}_j\}$$

$$\underline{U}_{ses} = Z_{ses} \cdot (P_{i-ses} - j \cdot Q_{i-ses}) / \underline{U}_i^* \quad (7)$$

$$I_{ses} = \frac{\underline{U}_i + \underline{U}_{ses} - \underline{U}_j}{Z_{ses}} = \frac{1}{Z_{ses}} \left(\underline{U}_i + Z_{ses} \cdot \frac{P_{i-ses} - j \cdot Q_{i-ses}}{\underline{U}_i^*} - \underline{U}_j \right), \quad (8)$$

where P_{i-ses} and P_{j-ses} are the active loads of the SSSC at nodes "i" and "j", and Q_{i-ses} and Q_{j-ses} are the reactive loads of the SSSC at nodes "i" and "j", respectively

As the UPFC is comprised of one series- and one shunt-voltage source its load model is obtained by applying both procedures described above; the shunt voltage source has the load equivalent explained with StatCom and the series source explained with SSSC. The procedure is illustrated in Fig. 4, which shows the original representation in a), the Norton equivalent in b) and the load equivalent in c). The relations between the representations for the UPFC are provided in equations (9) to (13). The currents of the shunt and series branches are provided in (14) and (15), respectively. They are needed for the control criteria (active and reactive power flow—see (25) and (26)) and the zero active power production criterion (see (23)).

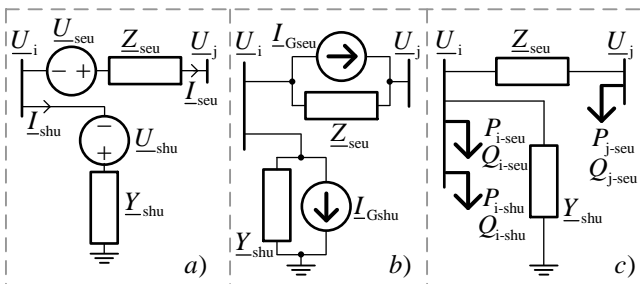


Fig. 4: Developing the UPFC load model.

$$I_{Gshu} = \underline{U}_{shu} \cdot \underline{Y}_{shu} \quad (9)$$

$$I_{Gseu} = \underline{U}_{seu} / Z_{seu} \quad (10)$$

$$P_{i-seu} = \text{Re}\{I_{Gseu}^* \cdot \underline{U}_i\}, \quad Q_{i-seu} = \text{Im}\{I_{Gseu}^* \cdot \underline{U}_i\}$$

$$P_{j-seu} = \text{Re}\{-I_{Gseu}^* \cdot \underline{U}_j\}, \quad Q_{j-seu} = \text{Im}\{-I_{Gseu}^* \cdot \underline{U}_j\} \quad (11)$$

$$P_{i-shu} = \text{Re}\{I_{Gshu}^* \cdot \underline{U}_i\}, \quad Q_{i-shu} = \text{Im}\{I_{Gshu}^* \cdot \underline{U}_i\}$$

$$\underline{U}_{shu} = (P_{i-shu} - j \cdot Q_{i-shu}) / (\underline{Y}_{shu} \cdot \underline{U}_i^*) \quad (12)$$

$$\underline{U}_{seu} = Z_{seu} \cdot (P_{i-seu} - j \cdot Q_{i-seu}) / \underline{U}_i^* \quad (13)$$

$$I_{shu} = (\underline{U}_i + \underline{U}_{shu}) \underline{Y}_{shu} = \left(\underline{U}_i + \frac{P_{i-shu} - j \cdot Q_{i-shu}}{\underline{Y}_{shu} \cdot \underline{U}_i^*} \right) \cdot \underline{Y}_{shu} \quad (14)$$

$$I_{seu} = \frac{\underline{U}_i + \underline{U}_{seu} - \underline{U}_j}{Z_{seu}} = \frac{1}{Z_{seu}} \left(\underline{U}_i + Z_{seu} \cdot \frac{P_{i-seu} - j \cdot Q_{i-seu}}{\underline{U}_i^*} - \underline{U}_j \right), \quad (15)$$

where P_{i-seu} and P_{j-seu} are active load equivalents of the UPFC series branch at nodes "i" and "j", and Q_{i-seu} and Q_{j-seu} are reactive loads equivalents of the UPFC series branch at nodes "i" and "j", and P_{i-shs} and Q_{i-shs} are active and reactive load equivalents of the shunt branch of the UPFC, respectively.

The active and reactive load powers of the above-described equivalents are the unknowns. They are bound to their correct values by a set of equations; we construct a vector function, which has the values of all its entries equal to zero, when the load powers are at their correct values for a given problem. The construction of the criterion function is explained next.

B. Construction of the criterion function

The criterion function is a statement, in equation form, of the physical constraints that accompany each device. We derive these equations so that all the quantities present in them are elements in a standard PF routine. Shunt and series voltage sources, which represent the FACTS devices (see Fig. 1), are not standard elements of PF routines and are therefore replaced by their load power equivalents.

The method proceeds by solving a system of equations, where the load powers present the unknowns and the entries of a criterion vector function are the equations. For a set of equations to be defined, the number of unknowns must equal the number of independent equations. Reviewing (2), (6) and (11) we can see that a StatCom provides two, an SSSC four and a UPFC six unknowns.

For *StatCom* we obtain the required two equations from the device's two physical conditions: the control F_{stm} , and the zero active power criterion. The active power of a StatCom, P_{stm} , is derived in (16). The control criterion is defined so that the device regulates the voltage magnitude of some node $|\underline{U}_{regs}|$ to the specified value U_{sps} and is stated in (17).

$$P_{stm} = \text{Re}\{\underline{U}_{shs} \cdot \underline{I}_{shs}^*\} = \frac{1}{(B_{shs}^2 + G_{shs}^2) \cdot |\underline{U}_i|^2} \left(G_{shs} \cdot (P_{i-shs}^2 + Q_{i-shs}^2) \right. \\ \left. + (G_{shs}^2 \cdot P_{i-shs} - B_{shs}^2 \cdot P_{i-shs} - 2 \cdot B_{shs} \cdot G_{shs} \cdot Q_{i-shs}) \cdot |\underline{U}_i|^2 \right) \quad (16)$$

$$F_{stm} = |\underline{U}_{regs}| - U_{sps}, \quad (17)$$

where G_{shs} is the real and B_{shs} is the imaginary part of \underline{Y}_{shs} .

For the SSSC, four equations are required. The first two are obtained in a similar manner as with the StatCom, i.e., we take the zero power criterion and the control criterion of the device. The active power production of an SSSC, P_{sc} , is derived in (18). The control criterion of the SSSC, F_{sc} , is defined so that the device controls the active power flow through its branch to the specified value, P_{sps} , and is provided in (19).

$$P_{sc} = \text{Re}\left\{\underline{U}_{ses} \cdot \underline{I}_{ses}^*\right\} = \frac{1}{|\underline{U}_i|^2 \cdot (R_{ses}^2 + X_{ses}^2)} \cdot \left((P_{i-ses}^2 + Q_{i-ses}^2) \cdot R_{ses} \cdot (R_{ses}^2 + X_{ses}^2) + |\underline{U}_i|^2 \cdot (2 \cdot Q_{i-ses} \cdot R_{ses} \cdot X_{ses} + P_{i-ses} \cdot (R_{ses}^2 - X_{ses}^2)) + |\underline{U}_i| |\underline{U}_j| \left((P_{i-ses} \cdot (X_{ses}^2 - R_{ses}^2) - 2 \cdot Q_{i-ses} \cdot R_{ses} \cdot X_{ses}) \cdot \cos(\delta_i - \delta_j) + (2 \cdot P_{i-ses} \cdot R_{ses} \cdot X_{ses} + Q_{i-ses} \cdot (X_{ses}^2 - R_{ses}^2)) \cdot \sin(\delta_i - \delta_j) \right) \right) \quad (18)$$

$$F_{sc} = \text{Re}\left\{\underline{U}_j \cdot \underline{I}_{ses}\right\} - P_{sps} = \frac{|\underline{U}_j|}{|\underline{U}_i| \cdot (R_{ses}^2 + X_{ses}^2)} \cdot (R_{ses} |\underline{U}_i| |\underline{U}_j| - (R_{ses} |\underline{U}_i|^2 + P_{i-ses} (R_{ses}^2 + X_{ses}^2)) \cos(\delta_i - \delta_j) - (|\underline{U}_i|^2 X_{ses} + Q_{i-ses} (R_{ses}^2 + X_{ses}^2)) \sin(\delta_i - \delta_j)) - P_{sps} \quad (19)$$

where R_{ses} is the real and X_{ses} is the imaginary part of Z_{ses} and δ_i and δ_j are the angles of their respective voltages.

The third and fourth equations of the SSSC are developed to ensure that the load powers are ascribable to a single series voltage source. From Fig. 3 we can see that the load powers are ascribable to the series voltage source when they are ascribable to the respective Norton equivalent. For this to be the case, the currents that the powers P_{i-ses} and Q_{i-ses} draw from node “i” must be the same as the currents that the powers P_{j-ses} and Q_{j-ses} push into node “j”. To construct two equations from the described condition, we take the current difference of the load powers at both nodes. As the current is complex, its real and its imaginary part each provide an equation. The current difference, $\Delta \underline{I}_{Gses}$, of the SSSC’s loads is:

$$\Delta \underline{I}_{Gses} = \left((P_{i-se} + j \cdot Q_{i-se}) / \underline{U}_i + (P_{j-se} + j \cdot Q_{j-se}) / \underline{U}_j \right)^* \quad (20)$$

The equations for the real and imaginary parts of (20) are:

$$\text{Re}\{\Delta \underline{I}_{Gses}\} = \frac{1}{|\underline{U}_i| |\underline{U}_j|} \cdot \left(|\underline{U}_i| \cdot (P_{j-ses} \cdot \cos(\delta_j) + Q_{j-ses} \cdot \sin(\delta_j)) + |\underline{U}_j| \cdot (P_{i-ses} \cdot \cos(\delta_i) + Q_{i-ses} \cdot \sin(\delta_i)) \right) \quad (21)$$

$$\text{Im}\{\Delta \underline{I}_{Gses}\} = \frac{1}{|\underline{U}_i| |\underline{U}_j|} \cdot \left(|\underline{U}_i| \cdot (P_{j-ses} \cdot \sin(\delta_j) - Q_{j-ses} \cdot \cos(\delta_j)) + |\underline{U}_j| \cdot (P_{i-ses} \cdot \sin(\delta_i) - Q_{i-ses} \cdot \cos(\delta_i)) \right) \quad (22)$$

Lastly, the UPFC must provide six equations. The first is the active power condition; the active power production of the UPFC, P_u , derived in (23), must remain zero.

The next three equations are the device’s control criteria

and are chosen as follows. The first control criterion, F_{u1} in (24), is the voltage magnitude at node “i”, which is to be kept at its specified value, U_{spu} . The second control criterion, F_{u2} shown in (25), is the control of the active power flow, to be kept at P_{spu} . The third control criterion, F_{u3} shown in (26), is the control of the reactive power flow, to be kept at Q_{spu} .

The final two equations of a UPFC, (27) and (28), are obtained from the necessity that the powers corresponding to the series source (P_{i-seu} , Q_{i-seu} , P_{j-seu} and Q_{j-seu}) stem from a single current source, as explained with the SSSC.

$$P_u = \text{Re}\left\{\underline{U}_{shu} \cdot \underline{I}_{shu}^* + \underline{U}_{seu} \cdot \underline{I}_{seu}^*\right\} = P_{i-shu} - P_{i-seu} - \frac{2B_{shu}^2 \cdot P_{i-shu}}{B_{shu}^2 + G_{shu}^2} + \frac{(P_{i-seu}^2 + Q_{i-seu}^2) \cdot R_{seu}}{U_i^2} + \frac{G_{sh} \cdot (P_{i-shu}^2 + Q_{sh} \cdot (Q_{sh} - 2B_{sh} \cdot U_i^2))}{(B_{shu}^2 + G_{shu}^2) \cdot U_i^2} + \frac{2R_{seu} \cdot (P_{i-seu} \cdot R_{seu} + Q_{i-seu} \cdot X_{seu})}{R_{seu}^2 + X_{seu}^2} + \frac{U_j}{U_i \cdot (R_{seu}^2 + X_{seu}^2)} \quad (23)$$

$$\left((2P_{i-seu} \cdot R_{seu} \cdot X_{seu} + Q_{i-seu} \cdot (X_{seu}^2 - R_{seu}^2)) \cdot \sin(\delta_i - \delta_j) + (P_{i-seu} \cdot (X_{seu}^2 - R_{seu}^2) - 2Q_{i-seu} \cdot R_{seu} \cdot X_{seu}) \cdot \cos(\delta_i - \delta_j) \right)$$

$$F_{u1} = |\underline{U}_i| - U_{spu} \quad (24)$$

$$F_{u2} = \text{Re}\left\{\underline{U}_j \cdot \underline{I}_{seu}\right\} - P_{spu} = \frac{|\underline{U}_j|}{|\underline{U}_i| \cdot (R_{seu}^2 + X_{seu}^2)} \cdot \left(R_{seu} |\underline{U}_i| |\underline{U}_j| - (R_{seu} |\underline{U}_i|^2 + P_{i-seu} (R_{seu}^2 + X_{seu}^2)) \cos(\delta_i - \delta_j) - (|\underline{U}_i|^2 X_{seu} + Q_{i-seu} (R_{seu}^2 + X_{seu}^2)) \sin(\delta_i - \delta_j) \right) - P_{spu} \quad (25)$$

$$F_{u3} = \text{Im}\left\{\underline{U}_j \cdot \underline{I}_{seu}\right\} - Q_{spu} = \frac{|\underline{U}_j|}{|\underline{U}_i| \cdot (R_{seu}^2 + X_{seu}^2)} \cdot \left(X_{seu} |\underline{U}_i| |\underline{U}_j| - (|\underline{U}_i|^2 \cdot X_{seu} + Q_{i-seu} \cdot (R_{seu}^2 + X_{seu}^2)) \cos(\delta_i - \delta_j) + (R_{seu} (P_{i-seu} \cdot R_{seu} + |\underline{U}_i|^2) + P_{i-seu} \cdot X_{seu}^2) \sin(\delta_i - \delta_j) \right) \quad (26)$$

$$\text{Re}\{\Delta \underline{I}_{Gseu}\} = \frac{1}{|\underline{U}_i| |\underline{U}_j|} \cdot \left(|\underline{U}_i| \cdot (P_{j-seu} \cdot \cos(\delta_j) + Q_{j-seu} \cdot \sin(\delta_j)) + |\underline{U}_j| \cdot (P_{i-seu} \cdot \cos(\delta_i) + Q_{i-seu} \cdot \sin(\delta_i)) \right) \quad (27)$$

$$\text{Im}\{\Delta \underline{I}_{Gseu}\} = \frac{1}{|\underline{U}_i| |\underline{U}_j|} \cdot \left(|\underline{U}_i| \cdot (P_{j-seu} \cdot \sin(\delta_j) - Q_{j-seu} \cdot \cos(\delta_j)) + |\underline{U}_j| \cdot (P_{i-seu} \cdot \sin(\delta_i) - Q_{i-seu} \cdot \cos(\delta_i)) \right) \quad (28)$$

The equations are inserted into a criterion function, which is a function of three vectors: the nodal voltage amplitudes and angles \mathbf{X} (these are the variables of the power mismatch formulated PF), the active and reactive loads that model the FACTS devices \mathbf{W} (see (30)), and the PF constants $\mathbf{\Theta}$ (these are the impedances and admittances, taps and phases, and all the other constant parameters that define the system). We can

write:

$$\begin{aligned} \mathbf{H}(\mathbf{X}, \boldsymbol{\Theta}, \mathbf{W}) = & \left[P_{\text{stm-1}}, F_{\text{stm-1}}, \dots, P_{\text{stm-Nst}}, F_{\text{stm-Nst}}, P_{\text{sc-1}}, F_{\text{sc-1}}, \right. \\ & \text{Re}\{\Delta I_{\text{Gses-1}}\}, \text{Im}\{\Delta I_{\text{Gses-1}}\}, \dots, P_{\text{sc-Nsc}}, F_{\text{sc-Nsc}}, \text{Re}\{\Delta I_{\text{Gses-Nsc}}\}, \\ & \text{Im}\{\Delta I_{\text{Gses-Nsc}}\}, P_{\text{u-1}}, F_{\text{u1-1}}, F_{\text{u2-1}}, F_{\text{u3-1}}, \text{Re}\{\Delta I_{\text{Gseu-1}}\}, \text{Im}\{\Delta I_{\text{Gseu-1}}\}, \\ & \left. \dots, P_{\text{u-Nu}}, F_{\text{u1-Nu}}, F_{\text{u2-Nu}}, F_{\text{u3-Nu}}, \text{Re}\{\Delta I_{\text{Gseu-Nu}}\}, \text{Im}\{\Delta I_{\text{Gseu-Nu}}\} \right]^T \end{aligned} \quad (29)$$

At this stage the modeling task can be restated as follows. We are to find the values \mathbf{W} , such that the value of \mathbf{H} becomes $\mathbf{0}$. We have reduced the task of modeling FACTS devices to finding the root of a system of equations. This root finding is based on the Newton method, as described in the following subsection. The function $\mathbf{H}(\mathbf{X}, \boldsymbol{\Theta}, \mathbf{W})$ is the criterion function and the vector \mathbf{W} defined in (30) is the control vector.

$$\begin{aligned} \mathbf{W} = & \left[P_{\text{i-shs-1}}, Q_{\text{i-shs-1}}, \dots, P_{\text{i-shs-Nst}}, Q_{\text{i-shs-Nst}}, P_{\text{i-ses-1}}, Q_{\text{i-ses-1}}, P_{\text{j-ses-1}}, \right. \\ & Q_{\text{j-ses-1}}, \dots, P_{\text{i-ses-Nsc}}, Q_{\text{i-ses-Nsc}}, P_{\text{j-ses-Nsc}}, Q_{\text{j-ses-Nsc}}, P_{\text{i-shu-1}}, Q_{\text{i-shu-1}}, \\ & P_{\text{i-seu-1}}, Q_{\text{i-seu-1}}, P_{\text{j-seu-1}}, Q_{\text{j-seu-1}}, \dots, P_{\text{i-shu-Nu}}, Q_{\text{i-shu-Nu}}, P_{\text{i-seu-Nu}}, \\ & \left. Q_{\text{i-seu-Nu}}, P_{\text{j-seu-Nu}}, Q_{\text{j-seu-Nu}} \right]^T \end{aligned} \quad (30)$$

C. Criterion Function Root Search using the Newton Method

As explained in the previous subsection the task of modeling FACTS devices is reduced to finding the values of the control vector \mathbf{W} that will correspond to the root of the criterion function \mathbf{H} . This is a multidimensional root-finding problem. We use the well-established Newton method for the root search. To use the Newton method, the first-order sensitivity of \mathbf{H} to changes in \mathbf{W} must be found. Partial derivatives do not readily provide the first-order sensitivity, since other variables of the power flow are also dependent on the loads of the system, i.e., \mathbf{X} is dependent upon \mathbf{W} . Full power system sensitivity [14] must be used as follows:

$$\frac{d\mathbf{H}}{d\mathbf{W}} = \frac{\partial \mathbf{H}}{\partial \mathbf{W}} + \frac{\partial \mathbf{H}}{\partial \mathbf{X}} \cdot \frac{d\mathbf{X}}{d\mathbf{W}} \quad (31)$$

In (31) the full derivative of \mathbf{X} with respect to \mathbf{W} ($d\mathbf{X}/d\mathbf{W}$) is defined by the PF itself. To develop an analytical expression for it we begin by viewing the power-flow problem in the power-mismatch form as a vector constraint. The constraint is essentially that the active power mismatch of the PQ- and PV-type nodes and the reactive power mismatch of the PQ-type nodes are kept at zero. We can write:

$$\mathbf{G}(\mathbf{X}, \boldsymbol{\Theta}, \mathbf{W}) = \mathbf{0} \quad (32)$$

The full derivative of (32) with respect to \mathbf{W} is zero since the function itself is a constant (zero). We can write:

$$\frac{d\mathbf{G}}{d\mathbf{W}} = \frac{\partial \mathbf{G}}{\partial \mathbf{W}} + \frac{\partial \mathbf{G}}{\partial \mathbf{X}} \cdot \frac{d\mathbf{X}}{d\mathbf{W}} = \mathbf{0} \quad (33)$$

From (33) and (31) we finally obtain:

$$\frac{d\mathbf{H}}{d\mathbf{W}} = \frac{\partial \mathbf{H}}{\partial \mathbf{W}} + \frac{\partial \mathbf{H}}{\partial \mathbf{X}} \cdot \left(\frac{\partial \mathbf{G}}{\partial \mathbf{X}} \right)^{-1} \cdot \frac{\partial \mathbf{G}}{\partial \mathbf{W}} \quad (34)$$

The construction of the derivative matrices in (34) must be carried out in accordance with the standard practices in matrix calculus [15], i.e., row size and positioning correspond to the vector being derived, while the column size and positioning correspond to the vector in the derivative's denominator.

With the full sensitivity of \mathbf{H} to changes in \mathbf{W} developed, the conditions for applying the Newton root search are met. At every iteration we update the vector \mathbf{W} as follows:

$$\mathbf{W}^{(k+1)} = \mathbf{W}^{(k)} - \left(\frac{d\mathbf{H}^{(k)}}{d\mathbf{W}^{(k)}} \right)^{-1} \cdot \mathbf{H}^{(k)}, \quad (35)$$

where the superscript (k) denotes the iteration number.

A stepwise procedure for the method is outlined below:

1. Assign value of \mathbf{W} from a flat start (the series voltage sources have 0 pu magnitude, while the shunt voltage sources have 1 pu magnitude at 180° angle).
2. Apply the current value of \mathbf{W} to the power-flow data (superimpose the loads on the original data) and run a full power-flow analysis, this obtains the values in vector \mathbf{X} (nodal amplitudes and angles).
3. Calculate the value of the criterion function \mathbf{H} for the last obtained values of \mathbf{W} and \mathbf{X} .
4. If the second norm of \mathbf{H} is sufficiently small, terminate and return the results. If not, proceed to step 5.
5. Calculate the sensitivity of \mathbf{H} with respect to \mathbf{W} for the last obtained values of \mathbf{X} and \mathbf{W} , as provided in (34).
6. Update \mathbf{W} according to the Newton method: $\mathbf{W}^{(k+1)} = \mathbf{W}^{(k)} - \left(\frac{d\mathbf{H}^{(k)}}{d\mathbf{W}^{(k)}} \right)^{-1} \cdot \mathbf{H}^{(k)}$, and go to step 2.

D. On Altering the Control Mode

The procedure for altering the control mode is straightforward and similar to that with other methods. To alter the control mode we alter the equation that provided it.

In (29) we can see that altering the control mode will alter the respective element of the criterion function \mathbf{H} . As the criterion function is altered, the partial derivatives of it (i.e., $\partial \mathbf{H}/\partial \mathbf{W}$ and $\partial \mathbf{H}/\partial \mathbf{X}$) are also altered. When calculating the sensitivity in (34) this has to be considered.

Putting it together: to alter a control mode we alter its respective equation (see (16), (19), (24), (25) and (26)), apply the appropriate changes to \mathbf{H} in (29), and recalculate the partial derivatives $\partial \mathbf{H}/\partial \mathbf{W}$ and $\partial \mathbf{H}/\partial \mathbf{X}$ used in (34).

E. On Considering Limitations

By foregoing the control mode and substituting its equation with another, the method can account for limitations. The procedure is related to the physical characteristics of the modeled devices and is used in other methods as well. For the sake of completeness it is repeated here.

Let the limitations be provided in a vector function $\boldsymbol{\Omega}$,

which is a function of the vectors \mathbf{X} , \mathbf{W} and Θ ;

$$\Omega = \Omega(\mathbf{X}, \Theta, \mathbf{W}) \quad (36)$$

If the n -th element of Ω exceeds its respective limit $\Omega_{n\text{-max}}$, we chose a control mode F_X (see (16), (19), (24), (25) and (26)) and redefine it as:

$$F_X = \Omega(n) - \Omega_{n\text{-max}}, \quad (37)$$

While for the StatCom and the SSSC device it is clear what should be done, the same does not hold for the UPFC—because the UPFC has three control modes the user must choose which control mode to forego if only one limitation of the device is exceeded. Choosing which UPFC control mode to forego must reflect the particular UPFC’s operational characteristics, which is up to the device’s designer.

The limitations of FACTS devices will generally not pertain to the variables directly used by the proposed method, but to the values present in the physical steady-state representation as shown in parts a) of Fig. 2–4. The quantities usually considered for the limitations are the angle or magnitude of a voltage source or the magnitude of the current flowing through a branch of a device. To consider the angle or magnitude of a voltage source we take either the angle or the absolute value of the respective equation among (3), (7), (12) and (13). Meanwhile, the current magnitude is obtained by taking the absolute value of the corresponding equation from among (4), (8), (14) and (15).

F. Applying Generalized and Non-Local Control Modes

With the application of smart grids and the information availability and control capability that ensue, on one hand, and the opposition to building new infrastructure, on the other, the system operator has both the motivation and the capability to use the controllable devices present in the system in unforeseen, possibly non-local, control modes. For example, the operator could use the degree of freedom provided by an SSSC to try and bring the line current of a nearby line or the voltage amplitude of a nearby node within limits. Future methods used to model FACTS devices will therefore have to be flexible in terms of altering the control mode.

The external character of the method presented, enables us to obtain the sensitivities of the control function \mathbf{H} to the control vector \mathbf{W} , numerically. This can be done by making small changes in \mathbf{W} , recording the resulting changes in \mathbf{H} and calculating the ratios between the respective changes. When altering the control modes, numerical evaluation of the derivatives can be used to ease the implementation, since it enables us to circumvent the calculation of the matrices in (34), which represent the crux of the method.

Numerical linearization will provide the full derivative, as long as the underlying system is continuous. This also makes the approach modular, meaning that another method can be used to model some FACTS devices in the underlying power-flow routine, while the method proposed here is used to model other FACTS devices with possibly different control modes.

The fact that numerical linearization provides the full derivative is not entirely obvious, it is however made clearer when revising the basic definition of the derivative:

$$\frac{df(x)}{dx} = \lim_{\Delta x \rightarrow 0} \frac{f(x + \Delta x) - f(x)}{\Delta x} \quad (38)$$

III. RESULTS

The method was tested on IEEE300 and Pegase13659 [16] bus systems. The underlying PF routine used was MatPower [17]. Both systems used are available in MatPower data.

All the shunt admittances of the StatCom (\underline{Y}_{shs}) and UPFC devices (\underline{Y}_{shu}) were $0.8 - 4i$ pu, which corresponds to an impedance of $5.8 + 29.1i \Omega$, and all the series impedances of the SSSC (\underline{Z}_{ses}) and UPFC (\underline{Z}_{seu}) devices were $0.05 + 0.25i$ pu, which corresponds to $6.1 + 30.2i \Omega$, both at a 110-kV base voltage level, with a 100-MVA base power.

The results section is separated into six subsections. Subsections A, B, and C test the modeling for one type of device and contain six cases each. The first five of these cases model a single device and the sixth case then tests the method for modeling all of the five devices, defined in the first five cases, operating at once. In subsection D, the method is tested on modeling several devices of different types operating at once. In subsection E, the use of numerical linearization is tested by having two UPFC devices performing non-local control. Lastly, subsection F tests the modeling of a large number of devices operating in a large system at once. The final case is carried out on the Pegase 13659 system, while all the other cases are carried out on the IEEE300 system.

A. Testing the StatCom modeling – IEEE300

Cases 1–5 test modeling of a single StatCom performing voltage control in the IEEE300 system. The input and solution data for these cases are shown in Table 1. The node of insertion is “node i ”, and “regs” is the regulated node. The iteration count for each case is provided in the column “iter.”.

In case 6, all five StatComs from cases 1–5 were inserted into the system at once. After six iterations the convergence is obtained. The solution is shown in Table 2.

Table 1: Input and solution data, StatCom, cases 1–5, IEEE300

Case	i	regs	$ \underline{U}_{shs} [\text{pu}]$	$\delta_{shs} [^\circ]$	iter.	$ \underline{U}_{sps} [\text{pu}]$
1	2	6	0.9870	-171.7	4	1.03
2	74	74	1.0391	157.6	2	1.00
3	129	129	0.9586	1761	2	1.00
4	175	175	1.1071	171.5	3	1.00
5	231	232	0.9635	-26.7	5	1.03

Table 2: Solution data for Statcoms, case 6, IEEE300

StatCom	From case	$ \underline{U}_{shs} [\text{pu}]$	$\delta_{shs} [^\circ]$
1	1	1.0087	172.3
2	2	1.2684	133.0
3	3	0.9620	160.1
4	4	1.1064	155.1
5	5	1.0096	-27.5

The iteration count for the first six cases shows that the

convergence for modeling StatComs is achieved quickly, both for single or multiple devices inserted in the system.

B. Testing the SSSC modeling – IEEE300

Cases 7–11 test the method for modeling a single SSSC device in the IEEE300 bus system. The input data and the solutions for these five cases are shown in Table 3.

In case 12, with five SSSC inserted at once, the calculation finished in five iterations. The results are shown in Table 4.

Table 3: Input and solutions data, SSSC, cases 7–11, IEEE300

Case	Line	$P_{\text{spu}}[\text{pu}]$	$ U_{\text{ses}} [\text{pu}]$	$\delta_{\text{ses}} [^\circ]$	iter.
7	40	-0.15	0.0775	-89.5	4
8	100	-0.40	0.1574	-110.6	4
9	200	-0.10	0.0515	-92.3	4
10	250	0.10	0.0836	85.0	4
11	310	0.25	0.0619	-171.4	4

Table 4: Solution data for SSSC devices, case 12, IEEE300

SSSC	From case	$ U_{\text{ses}} [\text{pu}]$	$\delta_{\text{ses}} [^\circ]$
1	7	0.0772	-90.1
2	8	0.1570	-111.0
3	9	0.0502	-93.2
4	10	0.0880	83.3
5	11	0.0615	-176.1

Cases 7–12 and their iteration count show that the method is able to model a single or several SSSC devices operating in the EPS at once with a low iteration count.

C. Testing the UPFC modeling – IEEE300

In cases 13–17, a single UPFC was modeled. The case parameters are shown in Table 5 and the solution in Table 6. In case 18 all five UPFC devices from the previous five cases are operating in the system at once. Convergence was obtained in six iterations. The results are shown in Table 7.

Table 5: Input data for cases 13–17, IEEE300

Case	Line	$P_{\text{spu}}[\text{pu}]$	$Q_{\text{spu}}[\text{pu}]$	$U_{\text{spu}}[\text{pu}]$
13	40	0.0	0.0	1.04
14	100	-1.5	0.0	1.02
15	200	0.0	-1.0	1.02
16	250	0.5	0.0	1.00
17	310	-0.5	0.0	0.98

Table 6: UPFC solution data for cases 13–17, IEEE300

Case	$ U_{\text{seu}} [\text{pu}]$	$\delta_{\text{seu}} [^\circ]$	$ U_{\text{shu}} [\text{pu}]$	$\delta_{\text{shu}} [^\circ]$	iter.
13	0.1266	-93.8	1.1028	-170.8	4
14	0.2639	51.4	1.0372	163.5	4
15	0.2958	178.5	0.8548	179.9	4
16	0.3015	-130.2	0.9488	169.2	6
17	0.2238	42.0	1.0474	153.3	4

Table 7: UPFC solution data for case 18, IEEE300 bus.

UPFC	From case	$ U_{\text{seu}} [\text{pu}]$	$\delta_{\text{seu}} [^\circ]$	$ U_{\text{shu}} [\text{pu}]$	$\delta_{\text{shu}} [^\circ]$
1	13	0.1267	-94.9	1.1029	-171.9
2	14	0.2643	50.5	1.0315	162.6
3	15	0.2959	177.0	0.8560	178.5
4	16	0.2985	-132.9	0.9498	166.8
5	17	0.2239	38.9	1.0474	150.2

The low iteration count in cases 13–18 indicates that the proposed method is suitable for modelling either a single or several UPFC devices operating in the system at once.

D. Modeling all three types of devices – IEEE300

Case 19 tests the method for modeling several devices of different types included at once, by inserting two devices of each type into the IEEE300 system. The calculation finished after five iterations. The data is provided in Table 8 and the voltage source solutions in Table 9. The low iteration count of this case illustrates that the method is applicable to scenarios where several FACTS devices of different types are installed.

Table 8: Case 19 input data, IEEE300 bus.

UPFC	Line	$P_{\text{spu}}[\text{pu}]$	$Q_{\text{spu}}[\text{pu}]$	$U_{\text{spu}}[\text{pu}]$
	40	-1.0	-1.5	1.03
	250	-0.5	0.0	1.00
SSSC	Line	$P_{\text{spu}}[\text{pu}]$		
	310	0.3		
	100	-0.4		
StatCom	Insertion node	Control node	$U_{\text{spu}}[\text{pu}]$	
	37	9001	1.00	
	129	133	1.00	

Table 9: Case 19 solution data, IEEE300 bus.

UPFC	Line	$ U_{\text{seu}} [\text{pu}]$	$\delta_{\text{seu}} [^\circ]$	$ U_{\text{shu}} [\text{pu}]$	$\delta_{\text{shu}} [^\circ]$
	40	0.4668	17.7	1.1142	-178.1
	250	0.6021	78.4	1.0519	153.4
SSSC	Line	$ U_{\text{ses}} [\text{pu}]$ <td colspan="2">$\delta_{\text{ses}} [^\circ]$</td>		$\delta_{\text{ses}} [^\circ]$	
	310	0.1583		-111.8	
	100	0.0850		-175.9	
StatCom	Insertion node	$ U_{\text{shs}} [\text{pu}]$ <td colspan="2">$\delta_{\text{shs}} [^\circ]$</td>		$\delta_{\text{shs}} [^\circ]$	
	37	0.8681		168.9	
	9004	0.8454		174.6	

E. Numerical linearization and non-local control – IEEE300

In case 20, two UPFC devices were inserted into the IEEE300 system to perform non-local control. The parameters for this case are shown in Table 10 for the first, and Table 11 for the second, UPFC. The solution is shown in Table 12.

Table 10: Case 20, input data for UPFC 1, IEEE300

Device location	Ctrl. mode	Type of control variable	Location of control variable	Specified value [pu]
Line # 162	F_{u1}	Voltage mag.	Node # 322	1.00
	F_{u2}	Active power	Line # 155	-0.10
	F_{u3}	Reactive power	Line # 155	0.00

Table 11: Case 20, input data for UPFC 2, IEEE300

Device location	Ctrl. mode	Type of control variable	Location of control variable	Specified value [pu]
Line # 332	F_{u1}	Voltage mag.	Node # 247	0.95
	F_{u2}	Voltage mag.	Node # 200	0.95
	F_{u3}	Reactive power	Line # 331	-0.05

Table 12: Case 20 solution, non-local control, IEEE300 bus.

UPFC	$ U_{\text{seu}} [\text{pu}]$	$\delta_{\text{seu}} [^\circ]$	$ U_{\text{shu}} [\text{pu}]$	$\delta_{\text{shu}} [^\circ]$
1	0.5360	75.6	0.9426	156.9
2	0.2260	-166.7	0.6599	164.0

F. Several devices, large case – Pegase 13659 bus

The last case tests the method on a much larger problem, i.e., inserting 3 StatCom, 4 SSSC, and 5 UPFC devices in the Pegase13659 bus system at once. The size of this case is unusually large; however, since the Pegase13659 system was designed to emulate the complexity of the European power system [16], this case tests the method for a scenario that might someday be required in real-world applications. The input data is shown in Table 13. The computation was finished in five iterations, which required 6.18 seconds on a personal computer with an Intel i5-2500 processor running at 3.30 GHz. The solution is shown in Table 14.

Table 13: Case 21 input data, PEGASE13,659 bus system.

	Line	P_{spu} [pu]	Q_{spu} [pu]	U_{spu} [pu]
	UPFC	1	1.0	0.0
10		0.0	1.0	1.03
100		-1.0	0.0	1.00
1'000		0.0	0.0	1.05
10'000		-1.0	0.0	1.05
	Line	P_{spu} [pu]		
	200	-0.1		
SSSC	2000	0.1		
	11000	-0.4		
	15000	0.0		
	Insertion node	Control node	U_{spu} [pu]	
	1000	5174	1.05	
StatCom	3000	2311	1.00	
	6000	13494	1.00	

Table 14: Case 21 solution data, PEGASE13,659 bus system.

	Line	$ U_{seu} $ [pu]	δ_{seu} [°]	$ U_{shu} $ [pu]	δ_{shu} [°]
	UPFC	1	0.2669	-99.9	1.1751
10		0.2975	135.7	0.9352	147.1
100		0.2762	17.3	0.8369	-10.7
1'000		0.1343	-131.9	0.9123	152.8
10'000		0.2851	93.5	1.1135	-170.0
	Line	$ U_{ses} $ [pu]	δ_{ses} [°]		
	200	0.0377	128.5		
SSSC	2000	0.0165	-132.6		
	11000	0.0059	80.6		
	15000	0.2355	-108.7		
	Insertion node	$ U_{shs} $ [pu]	δ_{shs} [°]		
	1000	0.9938	178.7		
StatCom	3000	1.0157	166.1		
	6000	1.0397	151.3		

IV. CONCLUSIONS AND REMARKS

A Newtonian method to model second-generation FACTS devices with unaltered PF programs is proposed. The method converges rapidly, even for an increased number of devices, as shown by tests on IEEE300 and PEGASE 13659 bus systems.

The external character of the method makes the sensitivities numerically attainable, which can be used to avert the first-order sensitivity calculation. This makes it easy to implement new and non-local control modes that might spur from the advent of smart-grid technologies. The numerical linearization for devices performing non-local control was tested in Section III. E. Since numerical linearization provides the full derivative, this also makes the method flexible. The underlying PF routine can be used to model some FACTS

devices, while the method described here is used to model other FACTS devices, possibly in unforeseen or non-local, control modes.

As the method is external to the PF it enables the user to switch to a different underlying PF routine, which could likely become available with recent advancements in embedding methods. Furthermore, since the proposed method relies on solving its own system of equations, the proposed method itself could benefit from these same embedding principles.

V. REFERENCES

- [1] W. F. Tinney and C. E. Hart, "Power Flow Solution by Newton's Method," *IEEE Trans. Power Appar. Syst.*, vol. PAS-86, no. 11, pp. 1449–1460, Nov. 1967.
- [2] A. Trias, "Fundamentals of the Holomorphic Embedding Load-Flow Method," *ArXiv150902421 Cs Math*, Sep. 2015.
- [3] A. Trias and J. L. Marin, "A Pade-Weierstrass technique for the rigorous enforcement of control limits in power flow studies," *ArXiv170704064 Cs*, Jul. 2017.
- [4] M. Basiri-Kejani and E. Gholipour, "Holomorphic Embedding Load-Flow Modeling of Thyristor-Based FACTS Controllers," *IEEE Trans. Power Syst.*, vol. 32, no. 6, pp. 4871–4879, Nov. 2017.
- [5] S. S. Baghsorkhi and S. P. Suetin, "Embedding AC Power Flow with Voltage Control in the Complex Plane: The Case of Analytic Continuation via Padé Approximants," *ArXiv150403249 Cs Math*, Mar. 2015.
- [6] A. Vinkovic and R. Mihalic, "Universal method for the modeling of the 2nd generation FACTS devices in Newton–Raphson power flow," *Int. J. Electr. Power Energy Syst.*, vol. 33, no. 10, pp. 1631–1637, Dec. 2011.
- [7] X.-P. Zhang, C. Rehtanz, and B. Pal, *Flexible AC Transmission Systems: Modelling and Control*, 2nd ed. 2012 edition. Berlin: Springer, 2012.
- [8] C. R. Fuerte-Esquivel and E. Acha, "A Newton-type algorithm for the control of power flow in electrical power networks," *IEEE Trans. Power Syst.*, vol. 12, no. 4, pp. 1474–1480, Nov. 1997.
- [9] S. D. Rao and D. J. Tylavsky, "Theoretical convergence guarantees versus numerical convergence behavior of the holomorphically embedded power flow method," *Int. J. Electr. Power Energy Syst.*, vol. 95, pp. 166–176, Feb. 2018.
- [10] S. Kamel and F. Jurado, "Fast decoupled load flow analysis with SSSC power injection model," *IEEJ Trans. Electr. Electron. Eng.*, vol. 9, no. 4, pp. 370–374, Jul. 2014.
- [11] Y. Zhang and Y. Zhang, "A novel power injection model of embedded SSSC with multi-control modes for power flow analysis inclusive of practical constraints," *Electr. Power Syst. Res.*, vol. 76, no. 5, pp. 374–381, Mar. 2006.
- [12] G. Bone and R. Mihalic, "Considering Controllable Devices Using Standard Load Flow programs – SSSC Example," *Int. J. Electr. Power Energy Syst.* - Accepted for publication on Jan 18. 2018.
- [13] G. Bone and R. Mihalic, "Comprehensive Tap and Phase Analysis in a framework external to the PF," *IEEE Transactions on Power Systems - Submitted for Publication on 20 Dec. 2017.*
- [14] J. Peschon, D. S. Piercy, W. F. Tinney, and O. J. Tveit, "Sensitivity in Power Systems," *IEEE Trans. Power Appar. Syst.*, vol. PAS-87, no. 8, pp. 1687–1696, Aug. 1968.
- [15] J. R. Magnus and H. Neudecker, *Matrix Differential Calculus with Applications in Statistics and Econometrics*, 2nd Edition, 2 edition. New York: Wiley, 1999.
- [16] C. Jozs, S. Fliscounakis, J. Maeght, and P. Panciatici, "AC Power Flow Data in MATPOWER and QCQP Format: iTesla, RTE Snapshots, and PEGASE," *ArXiv160301533 Math*, Mar. 2016.
- [17] R. D. Zimmerman, C. E. Murillo-Sanchez, and R. J. Thomas, "MATPOWER: Steady-State Operations, Planning, and Analysis Tools for Power Systems Research and Education," *IEEE Trans. Power Syst.*, vol. 26, no. 1, pp. 12–19, Feb. 2011.